Article

Toward a Magnetostructural Correlation for a Family of Mn SMMs

Constantinos J. Milios, Ross Inglis, Alina Vinslava, Rashmi Bagai, Wolfgang Wernsdorfer, Simon Parsons, Spyros P. Perlepes, George Christou, and Euan K. Brechin

J. Am. Chem. Soc., **2007**, 129 (41), 12505-12511• DOI: 10.1021/ja0736616 • Publication Date (Web): 22 September 2007

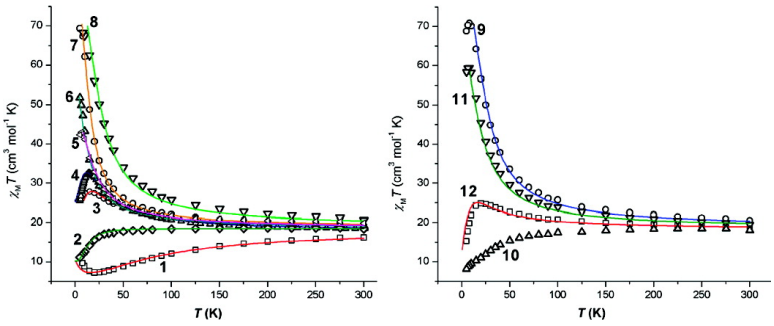

More About This Article

Additional resources and features associated with this article are available within the HTML version:

- Supporting Information
- Links to the 26 articles that cite this article, as of the time of this article download
- Access to high resolution figures
- Links to articles and content related to this article
- Copyright permission to reproduce figures and/or text from this article

View the Full Text HTML

J|A|C|S
ARTICLES
Published on Web 09/22/2007

Toward a Magnetostructural Correlation for a Family of Mn_6 SMMs

Constantinos J. Milios,[†] Ross Inglis,[†] Alina Vinslava,[§] Rashmi Bagai,[§] Wolfgang Wernsdorfer,[‡] Simon Parsons,[†] Spyros P. Perlepes,[||] George Christou,[§] and Euan K. Brechin*,[†]

Contribution from the School of Chemistry, The University of Edinburgh, West Mains Road, Edinburgh, EH9 3JJ, U.K., Laboratoire Louis Néel-CNRS, 38042 Grenoble, Cedex 9, France, Department of Chemistry, University of Florida, Gainesville, Florida 32611-7200, and Department of Chemistry, University of Patras, 26504 Patras, Greece

Received May 22, 2007; E-mail: ebrechin@staffmail.ed.ac.uk

Abstract: We have structurally and magnetically characterized a total of 12 complexes based on the Single-Molecule Magnet (SMM) $[Mn^{III}_6O_2(sao)_6(O_2CH)_2(MeOH)_4]$ (**1**) (where sao^{2-} is the dianion of salicylaldoxime or 2-hydroxybenzaldeyhyde oxime) that display analogous structural cores but remarkably different magnetic behaviors. Via the use of derivatized oxime ligands and bulky carboxylates we show that it is possible to deliberately increase the value of the spin ground state of the complexes $[Mn_6O_2(Me\text{-}sao)_6(O_2CCPh_3)_2(EtOH)_4]$ (**2**), $[Mn_6O_2(Et\text{-}sao)_6(O_2CCMe_3)_2(EtOH)_5]$ (**3**), $[Mn_6O_2(Et\text{-}sao)_6(O_2CPh^2OPh)_2(EtOH)_4]$ (**4**), $[Mn_6O_2(Et\text{-}sao)_6(O_2CPh^4OPh)_2(EtOH)_4(H_2O)_2]$ (**5**), $[Mn_6O_2(Me\text{-}sao)_6(O_2CPhBr)_2(EtOH)_6]$ (**6**), $[Mn_6O_2(Et\text{-}sao)_6(O_2CPh)_2(EtOH)_4(H_2O)_2]$ (**7**), $[Mn_6O_2(Et\text{-}sao)_6\{O_2CPh(Me)_2\}_2(EtOH)_6]$ (**8**), $[Mn_6O_2(Et\text{-}sao)_6(O_2C_{11}H_{15})_2(EtOH)_6]$ (**9**), $[Mn_6O_2(Me\text{-}sao)_6(O_2C\text{-}th)_2(EtOH)_4(H_2O)_2]$ (**10**), $[Mn_6O_2(Et\text{-}sao)_6(O_2CPhMe)_2(EtOH)_4(H_2O)_2]$ (**11**), and $[Mn_6O_2(Et\text{-}sao)_6(O_2C_{12}H_{17})_2(EtOH)_4(H_2O)_2]$ (**12**) ($Et\text{-}saoH_2$ = 2-hydroxypropiophenone oxime, $Me\text{-}saoH_2$ = 2-hydroxyethanone oxime, HO_2CCPh_3 = triphenylacetic acid, HO_2CCMe_3 = pivalic acid, HO_2CPh^2OPh = 2-phenoxybenzoic acid, HO_2CPh^4OPh = 4-phenoxybenzoic acid, HO_2CPhBr = 4-bromobenzoic acid, $HO_2CPh(Me)_2$ = 3,5-dimethylbenzoic acid, $HO_2C_{11}H_{15}$ = adamantane carboxylic acid, $HO_2C\text{-}th$ = 3-thiophene carboxylic acid, HO_2CPhMe = 4-methylbenzoic acid, and $HO_2C_{12}H_{17}$ = adamantane acetic acid) in a stepwise fashion from $S = 4$ to $S = 12$ and, in-so-doing, enhance the energy barrier for magnetization reorientation to record levels. The change from antiferromagnetic to ferromagnetic exchange stems from the "twisting" or "puckering" of the $(-Mn-N-O-)_3$ ring, as evidenced by the changes in the Mn−N−O−Mn torsion angles.

Introduction

The modern inorganic chemist can transform matter, not only for pleasure but for the design of new systems exhibiting desired physical or chemical properties.[1] Such an ambition, when dealing with the magnetic properties of polynuclear systems, necessitates going many times through the arcs of a cycle: (i) the synthesis of a new compound which one thinks will exhibit desirable magnetic properties, e.g., ferromagnetism; (ii) the determination of its molecular and crystal structure; (iii) the investigation of its magnetic properties, i.e., the determination of the sign and the strength of the exchange interactions, the value of the spin ground state and the nature and the relative energies of the low-lying energy states etc.;[2] (iv) the establishment of magnetostructural correlations; and (v) the theoretical analysis of the magnetostructural correlations, so that it becomes possible in the following cycle to synthesize novel compounds whose magnetic properties will be even closer to what is desired or expected. In the past 25 years, several research groups have shown that, by so doing, it is actually possible to improve (change) the nature and the order of magnitude of the interaction between the magnetic centers of certain *dinuclear* complexes.

It has long been recognized that for open-shell, ligand-bridged polymetallic compounds, some correlation must exist between the type and magnitude of magnetic interaction and the relative positions of the metal ions.[3] Magnetic studies on copper(II) acetate hydrate[4] and basic metal carboxylates[5] revealed antiferromagnetic interactions, from which their respective dinuclear and trinuclear structures, solved later,[6] were correctly predicted. "Real" magnetic studies on polynuclear metal complexes started in 1952 when Bleaney and Bowers[4] established a theoretical expression for the magnetic susceptibility of copper(II) acetate hydrate as a function of the temperature and the energy

[†] The University of Edinburgh.
[‡] Laboratoire Louis Néel-CNRS.
[§] University of Florida.
[||] University of Patras.

(1) Kahn, O. *Angew. Chem., Int. Ed. Engl.* **1985**, *24*, 834.
(2) (a) Anderson, P. W. *Phys. Rev.* **1959**, *115*, 2. (b) de Loth, P.; Cassoux, P.; Daudey, J. P.; Malrieu, J. P. *J. Am. Chem. Soc.* **1981**, *103*, 7124.
(3) Néel, L. *Compt. Rend.* **1936**, *203*, 304.
(4) Bleaney, B.; Bowers, K. D. *Proc. R. Soc. London* **1952**, *A214*, 451.
(5) Kambe, K. *J. Phys. Soc. Jpn.* **1950**, *5*, 48.
(6) (a) Van Niekerk, J. N.; Schoening, F. K. L. *Acta Crystallogr.* **1953**, *6*, 227. (b) Figgis, B. N.; Robertson, B. G. *Nature* **1965**, *205*, 694.

parameter J characterizing the interaction between the Cu^{II} centers within the molecule. By the mid-1970s numerous dinuclear and oligonuclear complexes had been synthesized, whose J-parameters were determined by comparing experimental magnetic susceptibility data with the appropriate theoretical laws.[7] More and more researchers then attempted to rationalize the sign and size of J in light of structural data. This allowed qualitative or quantitative correlations between structural and magnetic properties to be made (hence "magnetostructural correlations") and constituted an important step toward the understanding of the mechanism of interaction between metal centers.[1,8] The earliest of these correlations was established by Hatfield and Hodgson who showed a linear relationship between the magnetic parameter J and the Cu−O−Cu bridging angle φ in planar bis(μ-hydroxo) copper(II) dimers,[9,10] with the Cu−O distance being less important. The crossover from ferromagnetic to antiferromagnetic exchange occurs at approximately 97.5°. In the case of bis(μ-hydroxo)dichromium(III) complexes, both the Cr−O distance and the Cr−O−Cr angle are important; the major factor, however, seems to be the hybridization of the bridging oxygen atom, as reflected in the variation of the angle between the O−H vector and the Cr_2O_2 plane.[11] Other elegant correlations concerning bis(μ-halogeno)dicopper(II) compounds,[10,12] dinuclear copper(II) complexes with equatorial diazine/μ-1,1-azide bridge combinations,[13] (μ-oxo)diiron(III) species,[14] Fe^{III}_4 butterfly-type clusters,[15] and other dinuclear[16] and oligonuclear[17] systems were also established. These correlations have shown that the type and magnitude of the magnetic exchange interaction depends, in general, on the bridge identity, the metal−metal separation, the bond angles subtended at the bridging atoms, the dihedral angles between coordination planes containing the metal ions, the metal ligand bond lengths, and the metal ion stereochemistries.[13]

In recent years there has been a clear evolution from the initial studies in molecular magnetism[18] that addressed mostly dinuclear complexes, for which a detailed experimental and theoretical analysis of the correlation between structure and magnetic properties has been established, to polynuclear metal complexes or "clusters". Due to the increased structural complexity of clusters (especially so as the nuclearity increases) and the presence of many different exchange pathways in one molecule, a detailed study of the exchange interactions is often impossible. It should be recalled[15] that for large polynuclear metal complexes it may not be possible to extract a set of exchange coupling constants (J) from magnetic susceptibility data since (a) the size of the system and currently available computational resources may forbid fitting or simulation and (b) the existence of many solutions that perfectly fit the experimental data makes uncertain which is the physically acceptable set of J values. Thus, with a limited number of exceptions,[15a,17] magnetostructural correlations are unknown for clusters. Even less developed is theoretical analysis: despite the important role (and much recent success) that theoretical methods based on density functional theory can play in this field,[15] such studies have generally been employed to calculate J values (and to compare them with experimental data) or to help select a *"correct"* set of fitted values, rather than to obtain magnetostructural correlations, presumably due to the complexity of the systems.[19] Full analysis of magnetostructural correlations is also limited by the lack of theoretical models for clusters, in comparison with those employed for dinuclear complexes, for which the Hay−Thibeault−Hoffmann[20] and Kahn−Briat[21] models allow scientists to correlate J values with orbital energies and the overlap between magnetic orbitals, respectively. Notable exceptions are the recent studies on Fe^{III}_4 butterflies, in which a linear correlation between the "wing−body" interaction and the square of the overlap of the magnetic orbitals was found,[15] and on $Cu^{II}_4(\mu_3\text{-}O^-)_4$ cubanes, where the magnetic properties of the three subfamilies of such compounds (classified according to the number of short and long Cu···Cu distances present) were analyzed.[22]

Single-Molecule Magnets (SMMs)[23] are transition-metal clusters which have engaged the Molecular Magnetism community since their first appearance in 1993,[24] because their intrinsic properties promise access to the ultimate high-density memory storage device. Accordingly, the past 10 years has seen a rapid increase in the number of molecules which have been found to behave as SMMs, varying in nuclearity, topology, peripheral ligation, and metal.[25] The present paper describes our attempts at the *first* magnetostructural correlation for SMMs: we have expanded a particular structural type of Mn^{III}_6 SMMs into a family of related species that are invaluable in probing the various factors that affect the observed magnetic properties. We have studied the magnetic properties of the members of this family by analyzing the structural-dependence of the

(7) (a) Kato, M.; Jonassen, H. B.; Fanning, J. C. *Chem. Rev.* **1963**, *64*, 99. (b) Doedens, R. J. *Prog. Inorg. Chem.* **1975**, *19*, 173. (c) Martin, R. L. In *New Pathways in Inorganic Chemistry*; Ebsworth, E. A. V., Maddock, A., Sharpe, A. G., Eds.; Cambridge University Press: Cambridge, 1968.
(8) Gatteschi, D., Kahn, O., Willett, R. D., Eds. *Magneto-Structural Correlations in Exchange Coupled Systems*; D. Reidel: Dordrecht, 1985.
(9) Crawford, W. H.; Richardson, H. W.; Wasson, J. R.; Hodgson, D. J.; Hatfield, W. E. *Inorg. Chem.* **1976**, *15*, 2107.
(10) Hatfield, W. E. *Comments Inorg. Chem.* **1981**, *1*, 105.
(11) (a) Glerup, J.; Hodgson, D. J.; Petersen, E. *Acta Chem. Scand.* **1983**, *A37*, 161. (b) Charlot, M. F.; Kahn, O.; Drillon, M. *Chem. Phys.* **1982**, *70*, 177. (c) Hodgson, D. J. In *Magneto-Structural Correlations in Exchange Coupled Systems*; Gatteschi, D., Kahn, O., Willett, R. D., Eds.; D. Reidel: Dordrecht, 1985; pp 497−522.
(12) (a) Marsh, W. E.; Patel, K. C.; Hatfield, W. E.; Hodgson, D. J. *Inorg. Chem.* **1983**, *22*, 511. (b) Landee, C. P.; Greeney, R. E. *Inorg. Chem.* **1986**, *25*, 3371 (see also references therein).
(13) Tandon, S. S.; Thompson, L. K.; Manuel, M. E.; Bridson, J. N. *Inorg. Chem.* **1994**, *33*, 5555.
(14) (a) Gorun, S. M.; Lippard, S. J. *Inorg. Chem.* **1991**, *30*, 1625. (b) Weihe, H.; Güdel, H. U. *J. Am. Chem. Soc.* **1997**, *119*, 6539.
(15) (a) Cauchy, T.; Ruiz, E.; Alvarez, S. *J. Am. Chem. Soc.* **2006**, *128*, 15722. (b) Neese, F. *J. Am. Chem. Soc.* **2006**, *128*, 10213. (c) Pederson, M. R.; Khanna, S. N. *Phys. Rev. B* **1999**, *59*, 693 R. (d) Postnikov, A. V.; Kortus, J.; Pederson, M. R. *Phys. Status Solidi B* **2006**, *243*, 2533.
(16) (a) Melnik, M. *Coord. Chem. Rev.* **1982**, *42*, 269. (b) Kato, M.; Muto, Y. *Coord. Chem. Rev.* **1988**, *92*, 45. (c) Ohba, S.; Kato, M.; Tokii, T.; Muto, Y.; Steward, O. W. *Mol. Cryst. Liq. Cryst.* **1993**, *233*, 335.
(17) (a) Isele, K.; Gigon, F.; Williams, A. F.; Bernardinelli, G.; Franz, P.; Decurtins, S. *Dalton Trans.* **2007**, 332. (b) Halcrow, M. A.; Sun, J.-S.; Huffman, J. C.; Christou, G. *Inorg. Chem.* **1995**, *34*, 4167. (c) Clemente-Juan, J. M.; Chansou, B.; Donnadieu, B.; Tuchagues, J.-P. *Inorg. Chem.* **2000**, *39*, 5515.
(18) Kahn, O. *Molecular Magnetism*; Wiley-VCH: New York, 1993.
(19) Ruiz, E. *Struct. Bonding* **2004**, *113*, 71.
(20) Hay, P. J.; Thibeault, J. C.; Hoffmann, R. *J. Am. Chem. Soc.* **1975**, *97*, 4884.
(21) (a) Kahn, O.; Briat, B. *J. Chem. Soc., Faraday Trans. 2* **1976**, *72*, 268. (b) Kahn, O.; Briat, B. *J. Chem. Soc., Faraday Trans. 2* **1976**, 1441.
(22) Tercero, J.; Ruiz, E.; Alvarez, S.; Rodriguez-Fortea, A.; Alemany, P. *J. Mater. Chem.* **2006**, *16*, 2729.
(23) For reviews, see: (a) Aromi, G.; Brechin, E. K. *Struct. Bonding* **2006**, *122*, 1. (b) Bircher, R.; Chaboussant, G.; Dobe, C.; Güdel, H. U.; Ochsenbein, S. T.; Sieber, A.; Waldman, O. *Adv. Funct. Mater.* **2006**, *16*, 209. (c) Gatteschi, D.; Sessoli, R. *Angew. Chem., Int. Ed.* **2003**, *42*, 268. (d) Christou, G.; Gatteschi, D.; Hendrickson, D. N.; Sessoli, R. *MRS Bull.* **2000**, *25*, 66.
(24) Sessoli, R.; Tsai, H.-L.; Schake, A. R.; Wang, S.; Vincent, J. B.; Folting, K.; Gatteschi, D.; Christou, G.; Hendrickson, D. N. *J. Am. Chem. Soc.* **1993**, *115*, 1804.
(25) Aromí, G.; Brechin, E. K. *Struct. Bonding* **2006**, *122*, 1.

Scheme 1. Structural Formulas of the Main Ligands Discussed in the Text

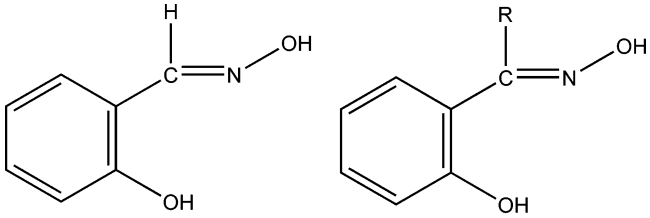

exchange coupling constants which control the ground-state spin. The outcome of our studies is a novel semiquantitative relationship that may even have consequences for a much broader family of Mn^{III} SMMs. It should be mentioned at this point that no magnetostructural correlation has been developed even for the heavily studied Mn_{12} family of SMMs.[23,25]

Experimental Section

Materials and Physical Measurements. All manipulations were performed under aerobic conditions using materials as received (reagent grade). ***Caution!*** Although we encountered no problems care should be taken when using the potentially explosive perchlorate anion. The derivitized oximes (Scheme 1) were synthesized as described elsewhere.[26] Complexes **1**, **3**, **7**, and **8** were synthesized as reported previously.[27] Variable temperature, solid-state direct current (dc) and alternating current (ac) magnetic susceptibility data down to 1.8 K were collected on a Quantum Design MPMS-XL SQUID magnetometer equipped with a 7 T dc magnet. Diamagnetic corrections were applied to the observed paramagnetic susceptibilities using Pascal's constants. Magnetic studies below 1.8 K were carried out on single crystals using a micro-SQUID apparatus operating down to 40 mK[28] and using a magnetometer consisting of a micro-Hall bar.

General Synthetic Methodology for Complexes 2, 4−6, 9−12. The formulae for all complexes reported herein are listed in Table 2. **Method 1.** To pale pink solutions of $Mn(ClO_4)_2 \cdot 6H_2O$ in MeOH (or EtOH) were added equivalent amounts of the derivitized oximes, the corresponding carboxylic acid, and CH_3ONa (or NEt_4OH). The solutions were left stirring for ~30 min, filtered, and then left to slowly evaporate. In each case suitable crystals grew after a period of 3−5 days. **Method 2.** The sodium salt of the corresponding carboxylic acid was treated with equivalent amounts of $Mn(ClO_4)_2 \cdot 6H_2O$, the derivitized oximes, and CH_3ONa (or NEt_4OH) in MeOH (or EtOH). Single crystals were grown upon slow evaporation. For all 12 compounds the yields vary from a minimum of 30% to a maximum of 50%.

X-ray Crystallography and Structure Solution. Diffraction data were collected at 150 K on a Bruker Smart Apex CCDC diffractometer, equipped with an Oxford Cryosystems LT device, using Mo radiation. See Table 1 and Supporting Information for full details.

Results and Discussion

Description of Structures. All complexes **1**−**12** display very similar molecular structures, and interatomic distances relevant to the discussion herein are shown in Table 2. All molecules possess an inversion center, besides complex **3** which lacks any molecular symmetry. They can be described (Figure 1) as consisting of two parallel off-set, stacked $[Mn^{III}_3(\mu_3\text{-O})]^{7+}$ triangular subunits linked *via* two "central" oximate O-atoms and two "peripheral" phenoxide O-atoms (O_{ph}), leading to a $[Mn^{III}_6(\mu_3\text{-O})_2(\mu_3\text{-ONR})_2(\mu\text{-ONR})_4]^{8+}$ core. The bridging between neighboring Mn ions within each triangle occurs through an NO oximate group, such that each Mn_2 pair forms a −Mn−N−O−Mn− moiety, and thus the Mn_3 triangle, a $(-Mn-O-N-)_3$ ring. In all complexes the coordination spheres of the Mn ions are completed by two terminal carboxylates (one on each triangle, except for complex **1** where the carboxylate (formate) is bridging in an $\eta^1{:}\eta^1{:}\mu$ fashion), by a phenoxide O-atom, and by terminal alcohol solvate molecules and/or H_2O molecules. All Mn ions are in the 3+ oxidation state, as confirmed by a combination of bond-length considerations, BVS calculations, and charge-balance. All are six-coordinate adopting distorted octahedral geometry, except for two Mn^{III} atoms in **1** (Mn3 and Mn3′) which are five-coordinate, adopting square-based pyramidal geometry. All Jahn−Teller (JT) axes are approximately coparallel, perpendicular to the $[Mn_3O]^{7+}$ planes.

Besides the carboxylate coordination mode, there are two other characteristic and important structural differences between the 12 reported complexes: (a) the distance between Mn3−O'_{ph} (and its symmetry equivalent, as shown in Figure 1) ranges from a minimum of 2.374 Å in **11** to a maximum of 3.524 Å in **1** (Table 2). This results in the formation of an extra bridge between the two triangular rings, which is present in **2**−**9** and **11** (2.374−2.492 Å), "weak" in **10** and **12** (2.519−2.619 Å), and absent in **1** (3.524 Å); (b) the Mn−O−N−Mn torsion angles (Table 3) within each triangular subunit range from a minimum value of 10.4° in **1** to a maximum value of 47.6° in **4**.

Dc Magnetic Susceptibility Studies: For all complexes direct current magnetic susceptibility studies were performed on polycrystalline samples in the 5−300 K temperature range under an applied field of 0.1 T. The results are plotted as the $\chi_M T$ product vs T in Figure 2 for complexes **1**−**8** and in Figure 3 for **9**−**12**.

For all complexes the $\chi_M T$ values at 300 K range from 18.38 to 20.57 $cm^3\ K\ mol^{-1}$, very close to the spin-only ($g = 2$) value of 18 $cm^3\ K\ mol^{-1}$ expected for a $[Mn_6]$ unit comprising six high-spin Mn^{III} ions. The only exception is complex **1** which displays a value of 16.19 $cm^3\ K\ mol^{-1}$. From Figures 2 and 3, it becomes clear that there are three different "categories" of magnetic behavior for **1**−**12**; the first corresponds to those complexes that display a general decrease in the $\chi_M T$ product upon cooling to smaller but nonzero values, i.e., complexes **1**, **2**, and **10** with low temperature $\chi_M T$ values of 10.39, 10.57, and 8.78 $cm^3\ K\ mol^{-1}$ at 5 K, respectively. This behavior is consistent with the presence of both antiferromagnetic and ferromagnetic interactions between the metal centers with the low-temperature values in each case indicating a relatively small ($S \approx 4$) spin ground state. The second category describes those complexes that display a constant increase in the $\chi_M T$ value upon cooling, reaching relatively high values at the lowest temperature studied, i.e., complexes **7**−**9** with values of 69.56, 69.53, and 69.50 $cm^3\ K\ mol^{-1}$ at 5 K, respectively. This behavior is consistent with the presence of only ferromagnetic interactions between the metal centers with the low-temperature value indicating an $S \approx 12$ ground state for each. The third

(26) Dunsten, W. R.; Henry, T. A. *J. Chem. Soc.* **1899**, *75*, 66.
(27) (a) Milios, C. J.; Vinslava, A.; Whittaker, A. G.; Parsons, S.; Wernsdorfer, W.; Christou, G.; Perlepes, S. P.; Brechin, E. K. *Inorg. Chem.* **2006**, *45*, 5272. (b) Milios, C. J.; Vinslava, A.; Wood, P. A.; Parsons, S.; Wernsdorfer, W.; Christou, G.; Perlepes, S. P.; Brechin, E. K. *J. Am. Chem. Soc.* **2007**, *129*, 8. (c) Milios, C. J.; Vinslava, A.; Wernsdorfer, W.; Moggach, S.; Parsons, S.; Perlepes, S. P.; Christou, G.; Brechin, E. K. *J. Am. Chem. Soc.* **2007**, *129*, 2754. (d) Milios, C. J.; Vinslava, A.; Wernsdorfer, W.; Prescimone, A.; Wood, P. A.; Parsons, S.; Perlepes, S. P.; Christou, G.; Brechin, E. K. *J. Am. Chem. Soc.* **2007**, *129*, 6547.
(28) Wernsdorfer, W. *Adv. Chem. Phys.* **2001**, *118*, 99.

Table 1. Crystallographic Data for Complexes **1**−**12**

	1·4MeOH	**2**·2EtOH	**3**	**4**	**5**·2MeOH
formula[a]	$C_{52}H_{64}Mn_6N_6O_{26}$	$C_{100}H_{108}Mn_6N_6O_{24}$	$C_{74}H_{102}Mn_6N_6O_{23}$	$C_{88}H_{90}Mn_6N_6O_{24}$	$C_{92}H_{112}Mn_6N_6O_{28}$
fw	1518.67	2107.55	1773.22	1945.28	2079.49
cryst syst	triclinic	monoclinic	triclinic	monoclinic	triclinic
space group	$P\bar{1}$	$C12/c1$	$P\bar{1}$	$I2/a$	$P\bar{1}$
T, K	150	150	150	150	150
λ, Å	Mo Kα (0.710 73)	Mo Kα (0.710 73)	Mo Kα (0.710 73)	Mo Kα (0.710 73)	Mo Kα (0.710 73)
a, Å	9.3612(3)	22.6018(4)	13.486(3)	21.074(10)	12.5755(5)
b, Å	12.8616(4)	15.0024(3)	14.882(3)	13.495(6)	13.1557(5)
c, Å	13.8655(5)	29.9529	20.822(4)	32.383(18)	15.3021(6)
α, deg	107.441(2)	90	82.87(3)	90	90.254(2)
β, deg	96.022(2)	106.8900(10)	85.73(3)	106.722(7)	92.248(2)
γ, deg	95.548(2)	90	76.51(3)	90	108.341(2)
V, Å^3	1569.4(1)	9718.4(3)	4027.6(15)	8820(7)	2400.74(16)
Z	1	4	2	4	1
ρ_{calcd}, g cm^{-3}	1.607	1.440	1.462	1.465	1.438
μ (Mo, Kα), mm^{-1}	1.257	0.833	0.988	0.911	0.845
measd/indep	25 771/8856	81 794/13 846	47 310/19 012	27 282/6354	37 251/13 342
(R_{int}) reflns	(0.031)	(0.062)	(0.056)	(0.1466)	(0.027)
obsd reflns [$I > 4\sigma(I)$]	6576	7315	10875	3803	10 948
R1[b]	0.0363	0.0394	0.0512	0.0815	0.0313
wR2	0.1063	0.0419	0.0282	0.0499	0.0849
GOF on F^2	0.965	1.1007	1.107	1.0028	0.9677
$\Delta\rho_{max,min}$, e Å^{-3}	0.72, −1.12	0.82, −0.50	0.90, −0.74	0.67, −0.71	0.58, −0.38

	6	**7**·2EtOH	**8**	**9**	**10**·2EtOH
formula[a]	$C_{74}H_{86}Br_2Mn_6N_6O_{24}$	$C_{80}H_{104}Mn_6N_6O_{26}$	$C_{84}H_{108}Mn_6N_6O_{24}$	$C_{88}H_{120}Mn_6N_6O_{24}$	$C_{70}H_{88}Mn_6N_6O_{26}S_2$
fw	1932.90	1895.30	1915.44	1961.40	1823.22
cryst syst	triclinic	triclinic	monoclinic	triclinic	triclinic
space group	$P\bar{1}$	$P\bar{1}$	$P21/n$	$P\bar{1}$	$P\bar{1}$
T, K	150	150	150	150	150
λ, Å	Mo Kα (0.710 73)	Mo Kα (0.710 73)	Mo Kα (0.710 73)	Mo Kα (0.710 73)	Mo Kα (0.710 73)
a, Å	12.2619(2)	12.4947(9)	12.9120(2)	12.7121(4)	11.1507(3)
b, Å	12.4095(3)	13.2846(9)	23.5530(4)	13.1980(4)	13.9643(3)
c, Å	14.2027(3)	14.5047(11)	15.1900(3)	15.2785(5)	14.3862(3)
α, deg	98.4370(10)	71.488(4)	90	75.593(2)	67.6930(10)
β, deg	90.7260(10)	82.305(4)	107.5490(10)	78.672(2)	70.4790(10)
γ, deg	104.6930(10)	68.687(4)	90	68.389(2)	75.7410(10)
V, Å^3	2065.03(8)	2126.4(3)	4404.53(14)	2292.53(13)	1934.91(8)
Z	1	1	2	1	1
ρ_{calcd}, g cm^{-3}	1.554	1.480(4)	1.444	1.421	1.565
μ (Mo, Kα), mm^{-1}	1.933	0.944	0.910	0.877	1.086
measd/indep	17 345/9801	49 242/11741	65 857/11 723	48 307/12 813	37 856/10 855
(R_{int}) reflns	(0.024)	(0.034)	(0.069)	(0.040)	(0.0573)
obsd reflns [$I > 4\sigma(I)$]	7855	8011	6207	8631	9148
R1[b]	0.0552	0.0339	0.0414	0.0426	0.0658
wR2	0.0646	0.1033	0.1425	0.0995	0.1473
GOF on F^2	1.0983	0.969	1.0197	0.8630	1.181
$\Delta\rho_{max,min}$, e Å^{-3}	2.70, −1.54	0.55, −0.45	1.42, −1.01	0.88, −0.94	1.318, −0.589

	11·2EtOH	**12**·2EtOH
formula[a]	$C_{82}H_{108}Mn_6N_6O_{26}$	$C_{90}H_{128}Mn_6N_6O_{26}$
fw	1923.35	2039.62
cryst syst	triclinic	triclinic
space group	$P\bar{1}$	$P\bar{1}$
T, K	150	150
λ, Å	Mo Kα (0.710 73)	Mo Kα (0.710 73)
a, Å	12.6159(3)	12.9841(3)
b, Å	13.0159(2)	13.2178(3)
c, Å	14.5850(3)	15.9543(4)
α, deg	105.6790(10)	77.164(2)
β, deg	92.6250(10)	69.3770(10)
γ, deg	105.1690(10	64.1280(10)
V, Å^3	2207.95(8)	2298.15(9)
Z	1	1
ρ_{calcd}, g cm^{-3}	1.446	1.474
μ (Mo, Kα), mm^{-1}	0.910	0.879
measd/indep	26 717/10 575	37 721/12 599
(R_{int}) reflns	(0.035)	(0.0321)
obsd reflns [$I > 4\sigma(I)$]	7652	9959
R1[b]	0.0366	0.0356
wR2	0.0892	0.0949
GOF on F^2	0.8861	1.053
$\Delta\rho_{max,min}$, e Å^{-3}	1.40, −0.78	0.461, −0.348

[a] $R_1 = \Sigma(|F_o| - |F_c|)/\Sigma(|F_o|)$. [b] $wR_2 = \{\Sigma[w(F_o^2 - F_c^2)^2]/\Sigma[w(F_o^2)^2]\}^{1/2}$.

category corresponds to complexes **3**−**6**, **11**, and **12**, which each display a slow or gradual increase in the value of $\chi_M T$ with decreasing temperature, with the low-temperature values "intermediate" between the two previous examples: 25.69, 25.72,

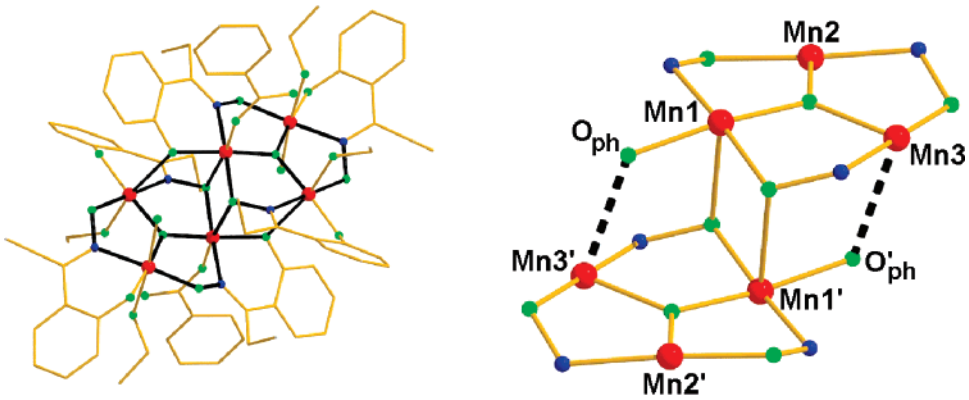

Figure 1. Molecular structure of **7** (left) and the general structural core observed in complexes **1**−**12** (right). Color code: Red = Manganese, Green = Oxygen, Blue = Nitrogen.

Table 2. Selected Interatomic Distances (Å) for Complexes **1**−**12**

complex	Mn1···Mn2	Mn2···Mn3	Mn1···Mn3	Mn3···O'_{ph}	Mn1···Mn1′
$[Mn_6O_2(sao)_6(O_2CH)_2(MeOH)_4]$ (**1**)	3.238(1)	3.258(1)	3.143(1)	3.524(2)	3.337(3)
$[Mn_6O_2(Me\text{-}sao)_6(O_2CCPh_3)_2(EtOH)_4]$ (**2**)	3.241(2)	3.263(2)	3.251(3)	2.384(2)	3.154(3)
$[Mn_6O_2(Et\text{-}sao)_6(O_2CCMe_3)_2(EtOH)_5]$ (**3**)[a]	3.256/3.247(3)	3.255/3.257(1)	3.271/3.246(3)	2.388/2.458(3)	3.341(2)
$[Mn_6O_2(Et\text{-}sao)_6(O_2CPh^2OPh)_2(EtOH)_4]$ (**4**)	3.232(2)	3.250(2)	3.248(2)	2.379(2)	3.231(3)
$[Mn_6O_2(Et\text{-}sao)_6(O_2CPh^4OPh)_2(EtOH)_4(H_2O)_2]$ (**5**)	3.260(2)	3.240(2)	3.268(1)	2.418(3)	3.213(1)
$[Mn_6O_2(Me\text{-}sao)_6(O_2CPhBr)_2(EtOH)_6]$ (**6**)	3.414(3)	3.233(1)	3.176(2)	2.492(3)	3.461(3)
$[Mn_6O_2(Et\text{-}sao)_6(O_2CPh)_2(EtOH)_4(H_2O)_2]$ (**7**)	3.257(2)	3.237(1)	3.280(3)	2.488(2)	3.229(1)
$[Mn_6O_2(Et\text{-}sao)_6\{O_2CPh(Me)_2\}_2(EtOH)_6]$ (**8**)	3.264(2)	3.247(3)	3.282(2)	2.480(2)	3.255(3)
$[Mn_6O_2(Et\text{-}sao)_6(O_2C_{11}H_{15})_2(EtOH)_6]$ (**9**)	3.262(1)	3.248(1)	3.282(1)	2.438(2)	3.221(1)
$[Mn_6O_2(Me\text{-}sao)_6(O_2C\text{-}th)_2(EtOH)_4(H_2O)_2]$ (**10**)	3.234(1)	3.238(1)	3.269(1)	2.619(2)	3.328(1)
$[Mn_6O_2(Et\text{-}sao)_6(O_2CPhMe)_2(EtOH)_4(H_2O)_2]$ (**11**)	3.257(2)	3.250(1)	3.273(1)	2.374(2)	3.266(1)
$[Mn_6O_2(Et\text{-}sao)_6(O_2C_{12}H_{17})_2(EtOH)_4(H_2O)_2]$ (**12**)	3.258(1)	3.224(1)	3.282(1)	2.519(1)	3.322(1)

[a] Complex **3** has no center of symmetry.

Table 3. Magnetostructural Parameters for Complexes **1**−**12**; Mn−N−O−Mn Torsion Angles *vs J* and *S*

complex	crystal system	space group	α/ deg	*J*/ cm^{-1} [a]	*S*[b]	1st exc. st. (cm^{-1})[c]	*g*[b]	*D*/ cm^{-1} [d]	τ_0/ s[e]	U_{eff}/ K[e]
1	triclinic	$P\bar{1}$	25.6, 18.0, 10.4	+1.25/−4.6/−1.8	4	3 (8)	1.99	−1.39	2.0×10^{-8}	28
2	monoclinic	*C*2/*c*	42.4, 25.5, 29.7	+1.2/−1.95	4	5 (10.5)	2.01	n.a.	6.8×10^{-10}	31.7
3	triclinic	$P\bar{1}$	42.1, 36.9, 23.3 42.2, 32.4, 16.7	+1.39/ −1.92	6	7 (0.5)	2.01	−0.75	3.0×10^{-8}	30
4	monoclinic	*I*2/*a*	47.6, 31.8, 23.7	+1.76/ −1.92	7	6 (0.1)	1.97	−0.39	1.5×10^{-10}	43.2
5	triclinic	$P\bar{1}$	43.7, 38.3, 30.3	+1.39/ −0.99	9	8 (0.03)	1.98	−0.37	1.2×10^{10}	56.9
6	triclinic	$P\bar{1}$	42.9, 31.9, 30.4	+1.15/ −0.73	11	12 (0.2)	1.98	−0.50	1.7×10^{-10}	50.2
7	triclinic	$P\bar{1}$	39.9, 38.2, 31.3	+0.93	12	11 (5)	1.99	−0.43	8.0×10^{-10}	53.1
8	monoclinic	*P*21/*n*	43.1, 39.1, 34.9	+1.63	12	11 (9)	1.99	−0.43	2×10^{-10}	86.4
9	triclinic	$P\bar{1}$	42.6, 36.7, 34.0	+1.60	12	11 (7.6)	1.99	−0.43	2.5×10^{-10}	79.9
10	triclinic	$P\bar{1}$	36.3, 31.1, 27.4	n.a.	n.a.	n.a.	n.a.	n.a.	n.a.	n.a.
11	triclinic	$P\bar{1}$	47.2, 38.2, 30.4	+1.85/−0.70	12	11 (1.4)	1.97	−0.44	7.5×10^{-10}	69.9
12	triclinic	$P\bar{1}$	41.5, 40.1, 27.8	+1.55/ −2.20	5 ± 1	4 (0.01)	1.98	n.a.	9.3×10^{-10}	31.2

[a] Calculated from dc susceptibility studies. [b]Calculated from both dc susceptibility and magnetization measurements. The latter were collected in the field and temperature ranges 0−7 T and 1.8−6 K. In each case the data were fit by a matrix-diagonalization method to a model that assumes only the ground state is populated, includes axial zero-field splitting ($D\hat{S}_z^2$), and carries out a full powder average. The corresponding Hamiltonian is $\hat{H} = D\hat{S}_z^2 + g\mu_B\mu_0\,\hat{S}\cdot H$ where *D* is the axial anisotropy, μ_B is the Bohr magneton, μ_0 is the vacuum permeability, $\hat{S}_z$ is the easy-axis spin operator, and *H* is the applied field (see ref 29c). [c]Calculated from dc susceptibility measurements. [d]Calculated from magnetization measurements. [e]Calculated from dc susceptibility data and/or single-crystal relaxation measurements performed on a micro-SQUID; n.a.= not available.

44.21, 53.51, 59.87, and 15.17 cm^3 K mol^{-1} at 5 K, respectively. This behavior is again diagnostic of competing ferro- and antiferromagnetic interactions within the cluster and is suggestive of "intermediate" spin ground states of $4 < S < 12$.

Despite their structural similarities, complexes **1**−**12** clearly display remarkably different magnetic behaviors, and in order to elucidate the origins of these differences we have simulated the susceptibility data for each. The best fit parameters from these are summarized in Table 3 and represented pictorially in Figures 2 and 3. For complex **1** the data were successfully simulated[29] employing the 3*J* model shown in Scheme 2a, using the spin Hamiltonian in eq 1. The calculated parameters were $J_1 = -1.8$ cm^{-1}, $J_2 = -4.6$ cm^{-1}, $J_3 = +1.25$ cm^{-1}, and $g = 1.99$. This leads to a ground state of $S = 4$ with the first excited state ($S = 3$) located 8 cm^{-1} above the ground state.[27a]

We were able to simulate the data for complex **3** using the 2*J* model shown in Scheme 2b and employing the spin

(29) (a) Borrás-Almenar, J. J.; Clemente-Juan, J. M.; Coronado, E.; Tsukerblat, B. S. *Inorg. Chem.* **1999**, *38*, 6081. (b) Borrás-Almenar, J. J.; Clemente-Juan, J. M.; Coronado, E.; Tsukerblat, B. S. *Comput. Chem.* **2001**, *22*, 985. (c) Piligkos, S.; Bill, E.; Collison, D.; McInnes, E. J. L.; Timco, G. A.; Weihe, H.; Winpenny, R. E. P.; Neese, F. *J. Am. Chem. Soc.* **2007**, *129*, 760.

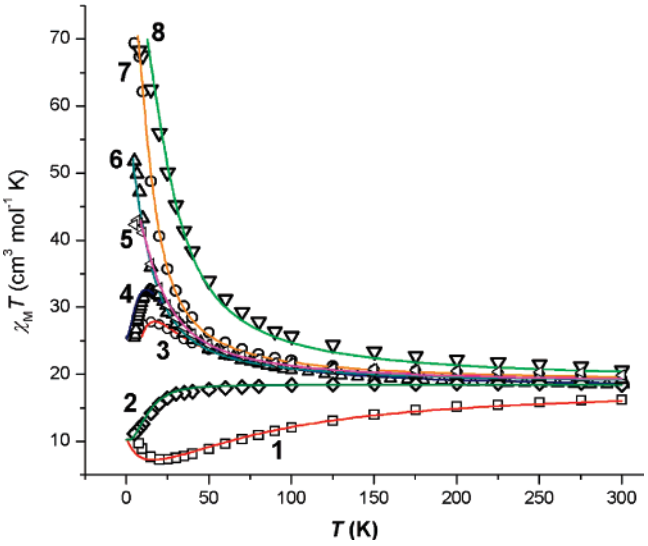

Figure 2. Plot of $\chi_M T$ *vs* T for complexes **1**−**8**. The solid lines represent simulations of the experimental data in the temperature range 300−5 K; see text for details.

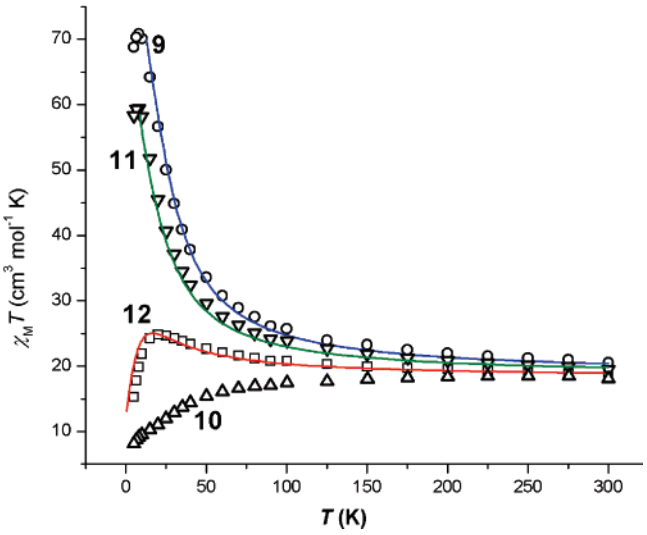

Figure 3. Plot of $\chi_M T$ *vs* T for complexes **9**−**12**. The solid lines represent simulations of the experimental data in the temperature range 300−5 K; see text for details.

Hamiltonian shown in eq 2. This afforded the parameters $J_1 = +1.39$ cm^{-1}, $J_2 = -1.92$ cm^{-1}, and $g = 2.01$. This results in a ground state of $S = 6$, but with the $S = 7$ and $S = 5$ excited states both located within 1 cm^{-1} of the ground state and an $S = 8$ state within 2.5 cm^{-1}.[27b] The interesting point here is that J_1 which corresponds to the interaction between two Mn ions bridged by an −N−O− moiety with torsion angles ranging from 32.4° to 42.2° has become ferromagnetic. In **1** where the torsion angles ranged from 10.4° to 25.6° the same interaction is antiferromagnetic.[27] We satisfactorily simulated the data for **7** using a simple 1*J*-model (Scheme 2c) despite the presence of (at least) two different interactions, and employing the spin Hamiltonian shown in eq 3. The parameters found were $J = +0.93$ cm^{-1} and $g = 2.00$, with $S = 11$ and $S = 10$ excited states 5 and 9 cm^{-1} above the $S = 12$ ground state, respectively. Now, with the torsion angles in **7** even larger than the ones observed in **3** and in **1** (31.3° to 39.9° for **7** vs 16.7° to 42.2° for **3** vs 10.4° to 25.6° for **1**), the complex displays ferromagnetic exchange and the maximum possible spin ground state. These results strengthened our initial speculation[27] that the twisting of the Mn−N−O−Mn moiety (or "puckering" of the Mn_3 triangle) was of vital importance in "switching" antiferromagnetic exchange to ferromagnetic exchange. Indeed we were able to simulate the data for all complexes (**1**−**12** (except **10**), Figures 2 and 3) using analogous exchange interaction patterns employed for **1**, **3**, and **7**. The torsion angles of these complexes (as shown in Figure 4) as well as the *S*, *J*, and *g* values for each are summarized in Table 3. From this data we can extract the following conclusions:

(i) In all cases the exchange *between* the Mn_3 triangles is ferromagnetic.

(ii) The exchange(s) within each Mn_3 triangle depend(s) solely on the individual Mn−O−N−Mn torsion angles; the larger the torsion angle, the more ferromagnetic the pairwise (Mn_2) interaction; the smaller the Mn−N−O−Mn torsion angle, the more antiferromagnetic the pairwise (Mn_2) interaction.

(iii) There is a *"magic area"* (30.4°−31.3°) for the torsion angles (α), less than 1° wide, above and below which we can predict the pairwise exchange to be ferro- or antiferromagnetic. That is, if $\alpha > 31.3°$, then $J > 0$ (F); if $\alpha < 30.4°$, then $J < 0$ (AF). When a Mn_3 triangle contains torsion angles that are both above and below this magic area, the data can only be simulated using both F and AF exchange, respectively.

(iv) It is the individual torsion angles between neighboring Mn ions that dictates the behavior of the complex, and *not* the average torsion angle, α_v. For example complex **2** has $\alpha_v = 32.5°$ but an $S = 4$ ground state; complex **7** has $\alpha_v = 36.5°$ and an $S = 12$ ground state; and complex **5** has $\alpha_v = 37.4°$ and an $S = 9$ ground state. This paradigm clearly shows the absence of any, at least linear, trend between average α_v values and *J*.

(v) The presence of the carboxylate in either coordinating mode (μ or terminally bonded) appears to have little effect on the sign of *J*. We previously speculated that the switching of the AF interactions in **1** to F interactions in **7** may be due, at least in some part, to the changing of the coordination mode of the carboxylate from μ-bridging (in **1**) to monodentate (in **7**), since the removal of the carboxylate bridge would presumably remove an antiferromagnetic contribution to the exchange between the Mn_2 pair.[27] However this appears not to be the case, and results here suggest the removal of the bridging carboxylate is not crucial in determining the sign of *J* between Mn_2 pairs. This is exemplified by complexes **1** and **10**, both of which display $S = 4$ ground states, despite the fact that the former contains a bridging carboxylate, and the latter, a terminal carboxylate.

(vi) If each Mn_2 exchange is ferromagnetic (i.e., an $S = 12$ complex), the larger the Mn−N−O−Mn torsion angle (α), the larger the barrier to magnetization relaxation (U_{eff}). For example, comparing complexes **7** and **9** (Table 3) with $J = +0.93$ cm^{-1} and $J = +1.60$ cm^{-1}, respectively, the U_{eff} values are 53.1 and 79.9 K. This presumably arises because an increase in torsion angle leads to an increase in $|J|$ which results in a more isolated ground state and a reduction in tunneling. This is reflected in the simulation of the susceptibility data. For example in complex **7** ($S = 12$) where $J = +0.93$ cm^{-1} the first excited state of $S = 11$ is located only 5 cm^{-1} above the ground state, whereas in complex **8** ($S = 12$) where $J = +1.65$ cm^{-1} the first excited state of $S = 11$ is located 9 cm^{-1} above the ground state, i.e., twice as high compared to **7**.

Scheme 2. Exchange Interaction Models Used for Complexes (a) **1**, (b) **3**, and (c) **7** and the Appropriate Spin-Hamiltonians Employed[a]

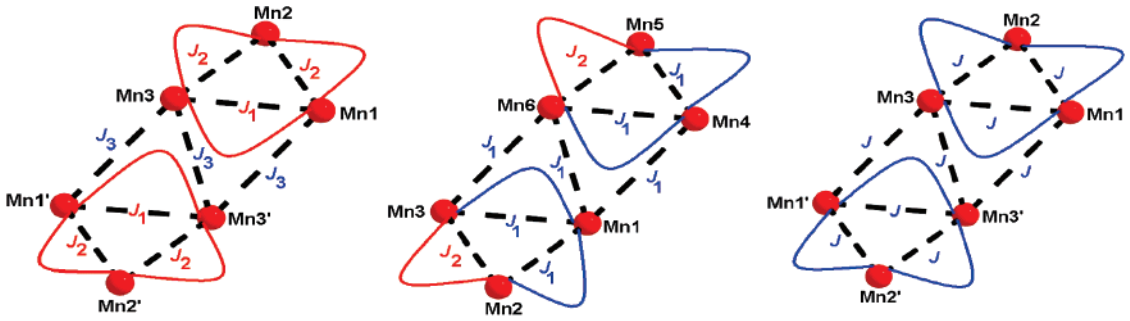

$$\hat{H} = -2J_1(\hat{S}_1\cdot\hat{S}_3 + \hat{S}_{1'}\cdot\hat{S}_{3'}) - 2J_2(\hat{S}_2\cdot\hat{S}_3 + \hat{S}_2\cdot\hat{S}_1 + \hat{S}_{2'}\cdot\hat{S}_{3'} + \hat{S}_{2'}\cdot\hat{S}_{1'}) - 2J_3(\hat{S}_3\cdot\hat{S}_{3'} + \hat{S}_3\cdot\hat{S}_{1'} + \hat{S}_{3'}\cdot\hat{S}_1) \quad (1)$$

$$\hat{H} = -2J_1(\hat{S}_1\cdot\hat{S}_2 + \hat{S}_1\cdot\hat{S}_3 + \hat{S}_1\cdot\hat{S}_4 + \hat{S}_3\cdot\hat{S}_6 + \hat{S}_3\cdot\hat{S}_4 + \hat{S}_6\cdot\hat{S}_4 + \hat{S}_5\cdot\hat{S}_4) - 2J_2(\hat{S}_3\cdot\hat{S}_2 + \hat{S}_6\cdot\hat{S}_5) \quad (2)$$

$$\hat{H} = -2J(\hat{S}_1\cdot\hat{S}_2 + \hat{S}_2\cdot\hat{S}_3 + \hat{S}_1\cdot\hat{S}_3 + \hat{S}_1\cdot\hat{S}_{2'} + \hat{S}_{2'}\cdot\hat{S}_{3'} + \hat{S}_{1'}\cdot\hat{S}_{3'} + \hat{S}_3\cdot\hat{S}_{1'} + \hat{S}_1\cdot\hat{S}_{1'} + \hat{S}_1\cdot\hat{S}_{3'}) \quad (3)$$

[a] Color code: blue line = ferromagnetic interaction, red line = antiferromagnetic interaction.

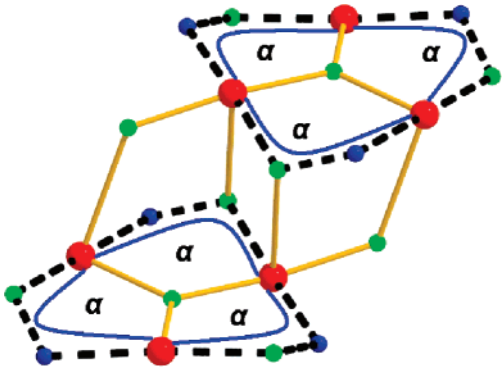

Figure 4. Mn−N−O−Mn core common to complexes **1**−**12**, highlighting the torsion angles (α) between Mn_2 pairs.

Conclusions

Although we still lack an exact quantitative mathematical expression, the above data clearly demonstrates that for this family of Mn_6 complexes it is possible not only to "control" and "understand" the nature of the spin ground state of a particular complex but also to predict the ground states of any new member of the Mn_6 family. Indeed it also allows us to speculate about the magnitude of the *J* values. The distortion of the torsion angles allows us to change the spin ground state from $S = 4$ to $S = 12$, in a stepwise fashion, passing through the $S = 5$, 6, 7, 9, and 11 intermediate ground states. We believe there are two fundamental reasons for what truly causes these structural distortions: (i) the bulky or "nonplanar" (alkyl) R-substituent on the derivatized oximes, since all derivatized analogues display larger torsion angles than complex **1** (non-derivatized), and (ii) the "bulkiness" of the carboxylate, exemplified by complexes **9** and **12** in which both complexes contain the same derivatized oxime (Et-saoH$_2$) but where their carboxylate ligands differ by only one additional $-CH_2$ group (adamantane$-COO^-$ vs adamantane$-CH_2-COO^-$). The additional $-CH_2$ group in **12** necessitates a small removal of the adamantane moiety from the $(-Mn-N-O-)_3$ ring resulting in less steric hindrance and less "twisting" or "puckering". This leads to a relaxation of the torsion angles (27.8° (**12**) versus 34.0° (**9**)) to below the "*magic area*" and thus to a smaller spin ground state ($S = 5 \pm 1$ for **12** versus $S = 12$ for **9**).

The above correlation is of course only valid for this family of Mn_6 complexes. However, we hope that the synthesis of new families containing the Mn/Rsao/RCO_2 blend will allow us to extend the validity of our system, the most obvious target being the synthesis of analogous Mn_3 triangles,[30] of which work is in progress. The effects of elegant structural distortion/modification on the physical properties of other SMMs, such as, for example, "Fe_4 stars",[31] "Fe_2Ni_2 squares",[32] "Mn_{25} barrels",[33] "Mn_4 cubanes",[34] and "Ni_4 cubanes"[35] has been rather subtle and has not always resulted in the enhancement of SMM properties or in the establishment of any magnetostructural correlation. For Mn_6 the effect is dramatic — a 3-fold increase in both *S* and U_{eff}.

We believe that the simple concept of targeted structural distortion must be valid for other systems and not simply applicable to derivatized salicylaldoximes in Mn(III) chemistry, and this is a hugely exciting prospect.

Supporting Information Available: Crystallographic information and magnetism data for **1**−**12**. This material is available free of charge via the Internet at http://pubs.acs.org.

JA0736616

(30) Stamatatos, T. C.; Foguet-Albiol, D.; Stoumpos, C. C.; Raptopoulou, C. P.; Terzis, A.; Wernsdorfer, W.; Perlepes, S. P.; Christou, G. *J. Am. Chem. Soc.* **2005**, *127*, 15380.
(31) Accorsi, S.; Barra, A.-L.; Caneschi, A.; Chastanet, G.; Cornia, A.; Fabretti, A. C.; Gatteschi, D.; Mortalo, C.; Olivieri, E.; Parenti, F.; Rosa, P.; Sessoli, R.; Sorace, L.; Wernsdorfer, W.; Zobbi, L. *J. Am. Chem. Soc.* **2006**, *128*, 4742.
(32) Li, D.; Clérac, R.; Wang, G.; Yee, G. T.; Holmes, S. M. *Eur. J. Inorg. Chem.* **2007**, 1341.
(33) Stamatatos, T. C.; Abboud, K. A.; Wernsdorfer, W.; Christou, G. *Angew. Chem., Int. Ed.* **2007**, *46*, 884.
(34) Andres, H.; Basler, R.; Güdel, H.-U.; Aromi, G.; Christou, G.; Buttner, H.; Ruffle, B. *J. Am. Chem. Soc.* **2000**, *122*, 12469.
(35) Yang, E.-C.; Wernsdorfer, W.; Zakharov, L. N.; Karaki, Y.; Yamaguchi, A.; Isidro, R. M.; Lu, G.-D.; Wilson, S. A.; Rheingold, A. L.; Ishimoto, H.; Hendrickson, D. N. *Inorg. Chem.* **2006**, *45*, 529.